Full Paper

IMPLEMENTATION OF ADVANCED CONTROL LAWS ON A LABORATORY-SCALE THREE-TANK SYSTEM

A. Bamimore
Department of Chemical Engineering, Obafemi Awolowo University, Ile-Ife, Nigeria.

K.S. Ogunba
Department of Electronic and Electrical Engineering, Obafemi Awolowo University, Ile-Ife, Nigeria.

M.A. Ogunleye
Department of Electronic and Electrical Engineering, Obafemi Awolowo University, Ile-Ife, Nigeria.

O. Taiwo
Department of Chemical Engineering, Obafemi Awolowo University, Ile-Ife, Nigeria.

A.S. Osunleke
Department of Chemical Engineering, Obafemi Awolowo University, Ile-Ife, Nigeria.

R. King
Head of Measurement and Control Group, Institute of Process and Plant Technology, Technical University of Berlin, Hardenberger, Berlin, Germany

ABSTRACT

A laboratory-scale three-tank system for Control Engineering Education has been installed at the Process System Engineering Laboratory of Obafemi Awolowo University, Ile-Ife, Nigeria. This study gives a description of the physical features of the three-tank system and the mathematical description of the dynamics of the system. Subsequently, the design and implementation of controllers using five popular advanced control laws are demonstrated. The performance of the designed control laws is displayed in set-point simulations using MATLAB and SIMULINK. The designs are then implemented on the physical system using the Real-Time Interface. The similarities observed between the experimental and simulation results show the effectiveness of the control systems and the usefulness of the set-up in demonstrating the practical relevance of advanced control laws.

Keywords: *Multivariable IMC, Method of Inequalities, Model Predictive Control, Three-Tank system, simplified decoupler*

1. INTRODUCTION

Together with well-known experimental control systems like the Quadruple-tank processes (Johanson, 2000; Vadigepalli *et al*., 2001; Shneiderman and Palmor, 2010; Garido *et al*., 2012), the Ball and Plate mechanism, the Inverted Pendulum, the electric servo-motor, the gyroscope, distillation column, the spring mass damper system, and the virtual boiler (Goodwin *et al*., 2000; Gatzke *et al*., 2000), a process of three interconnected tanks, the three-tank system (3TS), has emerged as a benchmark for laboratory demonstrations of control concepts, including illustrations of linear and nonlinear control and, more recently, the issues of fault detection, isolation and diagnosis and remote experimentation (Wu *et al*., 2003; Kovacs *et al*., 2007; Lincon *et al*., 2007; Klinkhieo and Patton, 2009; Suresh *et al*., 2009). The levels of water in two of the three tanks are controlled by the manipulation of the volumetric flow-rates delivered by two pumps. The third tank is observed but not controlled.

In this study, the nonlinear state equations relating the manipulated and controlled variables are stated. A linear model is obtained via a tangential linearization procedure around nominal operating point. The linear model is subsequently used to design controllers using a number of popular controller design techniques. These techniques are (i) Method-of-Inequalities-Synthesized Decentralized PI Control (ii) Full Multivariable Internal Model Control (iii) Simplified Decoupling Control (iv) Linear Model Predictive Control (v) H_∞-based Decentralized Control. The set-point tracking capabilities of the designed controllers are compared in simulation and experimental graphical plots.

1.1. Mathematical Preliminaries

The principal structure of the three tank plant is as shown in Figure 1. It is a two-input, two-output process in which the controlled variables are the levels h_1 and h_2 inside tanks 1 and 2 and the manipulated variables are the volumetric flow-rates of two pumps q_1 and q_2 respectively. The tank level h_3 of tank 3 is observed but not controlled.

The transient balance equations for all the tanks are,

$$A\frac{dh_1}{dt} = q_1 - q_{13} - d_1 \quad (1)$$

$$A\frac{dh_3}{dt} = q_{13} - q_{32} - d_3 \quad (2)$$

$$A\frac{dh_2}{dt} = q_2 + q_{32} - q_{20} - d_2 \quad (3)$$

where d_1, d_2, and d_3 represent leaks from tanks 1,2, and 3 respectively, A represents the cross-sectional area of the tanks, and q_{13}, q_{32}, and q_{20} are flow rates across pipes connecting, respectively, tanks 1 and 3, tanks 3 and 2, and tanks 2 and the water reservoir and are given by the Torricelli rule:

$$q_{13} = \mu_1 . S_p . sgn(h_1 - h_3) . \sqrt{2g|h_1 - h_3|} \quad (4)$$

$$q_{32} = \mu_3 . S_p . sgn(h_3 - h_2) . \sqrt{2g|h_3 - h_2|} \quad (5)$$

$$q_{20} = \mu_2 . S_p . \sqrt{2gh_2} \quad (6)$$

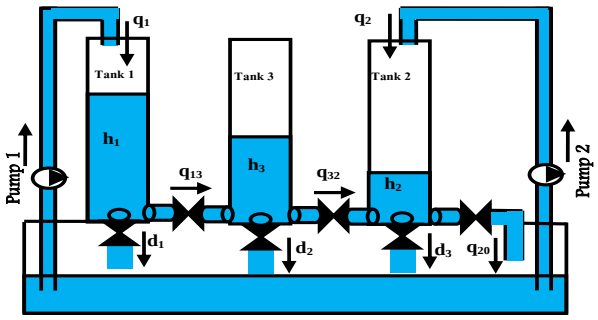

Figure 1: A Schematic of the Three-Tank System with Labels

with μ_i being the outflow coefficients out of tank $\boldsymbol{i}$, and $\boldsymbol{S_p}$ the cross-sectional area of the connecting pipes.

Making appropriate substitutions of equations (4) – (6) into equations (1) – (3) yields

$$\frac{dh_1}{dt} = -\left(1/_A\right).\mu_1.S_p.\sqrt{2g}.sgn(h_1-h_3).\sqrt{|h_1-h_3|} + \left(q_1/_A\right) - \left(d_1/_A\right) \quad (7)$$

$$\frac{dh_2}{dt} = \left(1/_A\right).\mu_3.S_p.\sqrt{2g}.sgn(h_3-h_2).\sqrt{|h_3-h_2|} - \left(1/_A\right).\mu_2.S_p.\sqrt{2g}.sgn(h_2).\sqrt{|h_2|} + \left(q_2/_A\right) - \left(d_2/_A\right) \quad (8)$$

$$\frac{dh_3}{dt} = \left(1/_A\right).\mu_1.S_p.\sqrt{2g}.sgn(h_1-h_3).\sqrt{|h_1-h_3|} - \left(1/_A\right).\mu_3.S_p.\sqrt{2g}.sgn(h_3-h_2).\sqrt{|h_3-h_2|} - \left(d_3/_A\right) \quad (9)$$

Linearizing the model equations (7)-(9) around the operating conditions given in equation (10).

$$\left.\begin{array}{c} h_{10} = 37.749, h_{20} = 15.145, h_{30} = 26.97 \\ \mu_{10} = 0.44, \mu_{20} = 0.87, \mu_{30} = 0.42 \\ q_{10} = 32\frac{cm^3}{s}, q_{20} = \frac{43cm^3}{s} \end{array}\right\} \quad (10)$$

yields linear model equation in s-domain.

$$\begin{bmatrix}\delta h_1 \\ \delta h_2\end{bmatrix} = \begin{bmatrix}g_{11} & g_{12} \\ g_{21} & g_{22}\end{bmatrix}\begin{bmatrix}\delta q_1 \\ \delta q_2\end{bmatrix} + \begin{bmatrix}g_{d11} & g_{d12} & g_{d13} \\ g_{d21} & g_{d22} & g_{d23}\end{bmatrix}\begin{bmatrix}\delta d_1 \\ \delta d_2 \\ \delta d_3\end{bmatrix} \quad (11)$$

$G(s)$ and $G_d(s)$ are used to denote the first and second terms of equation (11) and are defined as process and disturbance transfer functions respectively, given by:

$$\left.\begin{array}{l} g_{11} = \frac{0.006711s^2+0.0003003s+0.000002731}{s^3+0.05471s^2+0.0007534s+0.000001504} \\ g_{12} = \frac{6.072}{s^3+0.05471s^2+0.0007534s+0.000001504} \\ g_{21} = \frac{6.072}{s^3+0.05471s^2+0.0007534s+0.000001504} \\ g_{22} = \frac{0.000006072+0.0001946s+0.006711s^2}{s^3+0.05471s^2+0.0007534s+0.000001504} \end{array}\right\} \quad (12)$$

$$\left.\begin{array}{l} g_{d11} = \frac{-0.006711s^2-0.0003001s+0.000002726}{s^3+0.05471s^2+0.0007534s+0.000001504} \\ g_{d12} = \frac{-0.0000006068}{s^3+0.05471s^2+0.0007534s+0.000001504} \\ g_{d13} = \frac{-0.000006678s-0.000001714}{s^3+0.05471s^2+0.0007534s+0.000001504} \\ g_{d21} = \frac{-0.0000006068}{s^3+0.05471s^2+0.0007534s+0.000001504} \\ g_{d22} = \frac{-0.006711s^2-0.0001945s-0.0000006068}{s^3+0.05471s^2+0.0007534s+0.000001504} \\ g_{d23} = \frac{-0.00006099s-0.0000006068}{s^3+0.05471s^2+0.0007534s+0.000001504} \end{array}\right\} \quad (13)$$

2. Physical Layout of the Three-Tank System

The process being controlled in this experimental set-up is the three-tank plant shown in Figure 2, a combination of three transparent calibrated cylindrical Plexiglas tanks of equal dimensions. These tanks are connected together by cylindrical pipes with cross-sectional areas of $0.5\ cm^2$. The cross-sectional area of each tank is approximately $154\ cm^2$, while the maximum height of each tank is $62\ cm$ $(+/-1\ cm)$. The leftmost tank is labeled "tank 1," the middle tank "tank 3," and the rightmost tank "tank 2". The objective is to control the water levels of tanks 1 and 2 by the specification of reference command signals that ultimately results in the corresponding reaction of two diaphragm pumps.

Special differential pressure sensors are positioned behind each of the tanks to sense the levels of water in each of the three tanks. These differential pressure sensors sense the pressure differences between particular levels of water and a reference pressure level, and convert these pressure differentials into analog voltage values. An actuator device accepts signals from the sensors for Analog-to-Digital conversion before the digitized signals can be appropriately processed by the controlling equipment.

The controlling platform is a computer with a digital processing board, the dSPACE DS1104 R&D Controller Board. The board receives compiled codes from the computer and sends out a digital output signal to the AMIRA Actuator Device that corresponds to the control methodology's expected output unto a real system. This digital signal is then converted to an analog signal for transmission to the pumps.

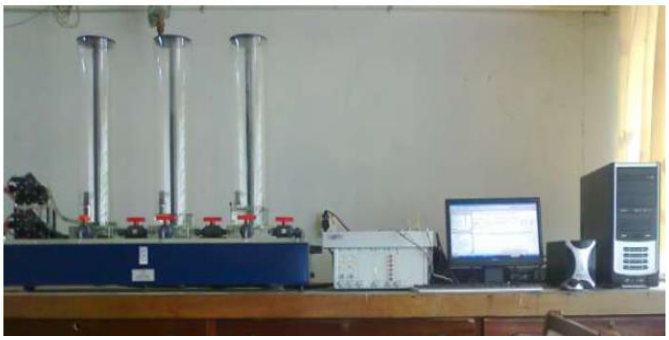

Figure 2: The Laboratory-Scale Three-Tank System for Real-Time Tank Height Control

Figure 3 gives the feedback representation of the components of the three-tank system set-up.

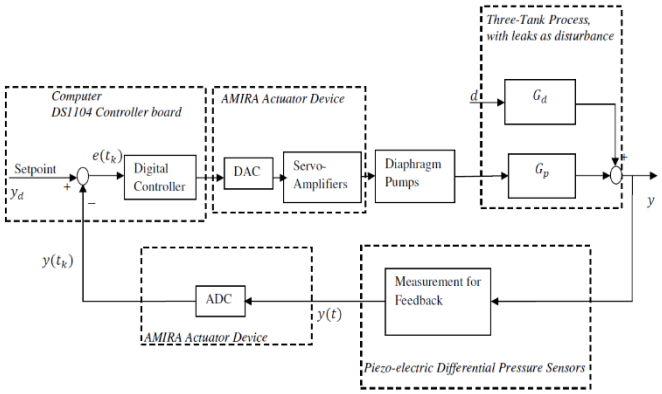

Figure 3: The Feedback Representation of the Components of the Three-Tank System Set-up

3. Input-Output Controllability Analysis

Here, simple analytical tools available are utilized to assess the controllability of the plant in order to evaluate any inherent performance limitations.

Scaling: While RGA, poles and zeros are independent of scaling, some other measures like singular values depend on it. All outputs,

set-points, inputs and disturbances are scaled by their "maximum acceptable deviation" from the desired operation conditions, such that the scaled variables stay within $\pm 1 \; \forall \; w$. The values used for scaling are given in (14) below:

$$\left.\begin{aligned} y_{maxdev} &= [h_1 \quad h_2] = [5 \quad 5] \\ u_{maxdev} &= [q_1 \quad q_2] = [53 \quad 43] \\ d_{maxdev} &= [d_1 \quad d_2 \quad d_3] = [20 \quad 20 \quad 20] \end{aligned}\right\} \tag{14}$$

Multivariable Interactions: Both the steady state relative gain array (RGA) and frequency dependent RGA were computed for the system to assess the level of interactions within the variables not only at steady state but at all frequencies. The steady state RGA is calculated as:

$$RGA = \begin{matrix} 1.29 & -0.29 \\ -0.29 & 1.29 \end{matrix} \tag{15}$$

It is clear that the interactions among the controlled variables are not so strong, meaning that the system is relatively decoupled. This indicates that decentralized control could be used with pairings $[h_1 \;\; q_1]$ and $[h_2 \;\; q_2]$.

The RGA elements as function of frequency are shown in Figure 4 reveal that the RGA elements decrease as frequency increases with almost negligible interactions at frequency greater than 0.1 rad/sec.

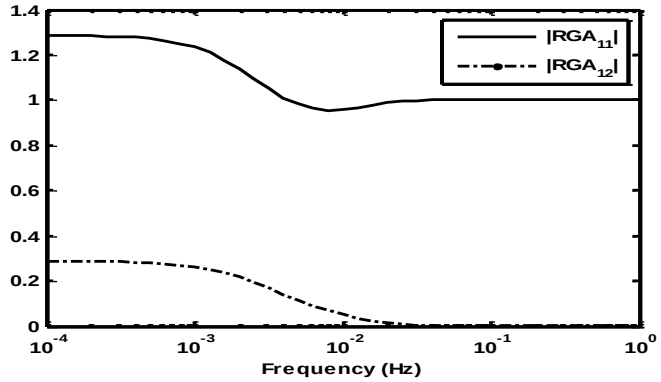

Figure 4: Input-Output controllability analysis: Frequency dependent RGA plot

Minimum-Phase (MP) Characteristics: The individual elements in the transfer function matrix have no right half plane (RHP) zeros. The multivariable transmission zeros of the process were equally calculated to be: $z_1 = -0.0024$, $z_2 = -0.018$ and $z_3 = -0.0336$, which shows that the process has no multivariable right half plane (RHP) zeros.

Sensitivity to Uncertainty: The condition number $\gamma(G)$ of the plant is plotted in Figure 5. It is of low order of magnitude indicating that the plant is not ill-conditioned. It is also higher at low frequency showing that the plant is more sensitive to unstructured uncertainty at steady state than at higher frequencies.

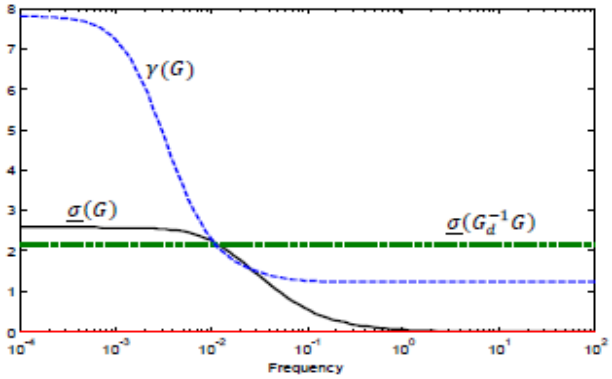

Figure 5: Input-output controllability analysis: Plots of $\underline{\sigma}(G), \gamma(G)$ and $\underline{\sigma}(G_d^{-1}G)$.

Functional Controllability: The system is functionally controllable as det[G(s)]≠ 0, ∀s .

Controllability (l): Consider a system m by m with transfer function G(s) whose McMillan standard form is

$$M(s) = diag\left(\epsilon_i(s) \Big/ \psi_i(s) \right), i = 1,2, \dots, m$$

where $\epsilon_i(s)$ and $\psi_i(s)$ are polynomials in s, G(s) is controllable if it is functionally controllable and none of the $\epsilon_i(s)$, has a zero in the closed loop. This plant satisfies this condition.

Modal Controllability (m): The condition here is that, matrix $[(sI - A), B]$ should be relatively left prime. This plant also satisfies this condition.

Input Saturation: Input saturation imposes a fundamental limitation on the control performance. The perfect control condition for reference tracking is given by:

$$\underline{\sigma}(R^{-1}G) \geq 1 \; \forall \; \omega \leq \omega_r \tag{16}$$

ω_r is the frequency up to which reference tracking is required. R is reference scaling matrix chosen as $R = I$. The condition for perfect disturbance rejection is given by (17) where $\boldsymbol{G_d}$ is the disturbance transfer function matrix.

$$\underline{\sigma}(G_d^{-1}G) \geq 1 \; \forall \; \omega \tag{17}$$

As shown in Figure 5, the minimum singular value of the plant, for reference tracking, is greater than 1 up to a frequency of $\omega = 0.046$. This is an upper bound on the controller bandwidth, ω_c due to input saturation considerations at high frequency. For disturbance rejection, the minimum singular value is greater than 1 at all frequencies, this shows that input saturation is not a serious problem for this plant.

4. Controller Design

In this work, the following control algorithms were considered for the control of the three-tank-system:

4.1. Multi-Objective Parameter Search for Multiloop PI Controller Design by Method of Inequalities (MoI)

The determination of controller parameters for multiloop Proportional-Integral (PI) controllers for the three-tank system was done using a multi-objective parameter-search optimization procedure called the Method of Inequalities (MoI) (Zakian and Al-Naib, 1973). The performance objectives were formulated as a set of algebraic inequalities

$$\phi_i(p) \leq \varepsilon_i, i = 1,2 \tag{18}$$

where $\phi_i(p)$ are objective functions for the two loops specified as functional of performance indices such as rise time, settling time, overshoot, stability margin, p is a vector $(p_1, p_2, \dots, p_q)$, and ε_i are real numbers chosen to limit the values of the objective functions.

Using the moving boundaries method with IMC parameterizations (Zakian and Al-Naib, 1973; Taiwo, 1978; Taiwo, 1980; Ogunleye, 2012), the PI controllers obtained are given by

$$g_{c1} = \left(23.79 + \frac{0.0608}{s}\right), g_{c2} = \left(39.81 + \frac{0.2202}{s}\right) \tag{19}$$

The comparisons of the set-point tracking manipulated and controlled variable plots of the experimental and simulation results for the implementation of the controllers of (19) are shown in Figure 6. The similarities between both plots are noteworthy.

4.2. Fixed-Structure $\mathbf{H}_\infty$ controller design

Here a H_∞ controller synthesis problem posed in equation 20 is solved as implemented in the MATLAB subroutine "hinfstruct".

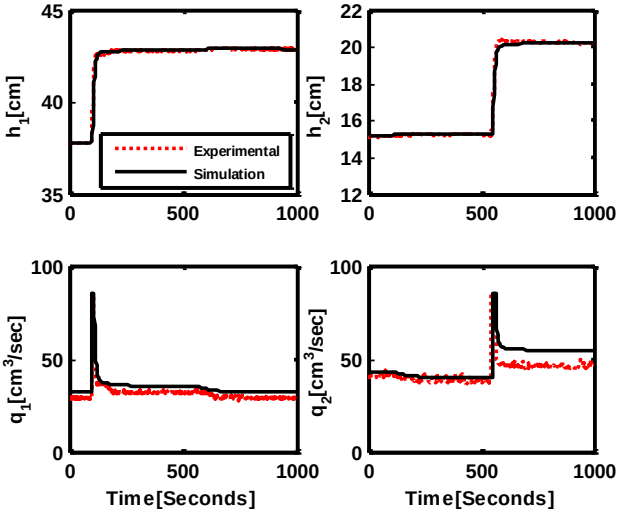

Figure 6: Setpoint Tracking Manipulated and Controlled Variable Plots of the Experimental and Simulation Results for the Implementation of the MoI-synthesized PI Controllers of (19)

$$\|\mathrm{H}(s)\|_\infty := \max_\omega \bar{\sigma}(\mathrm{H}(\mathrm{j}\omega)) < 1 \tag{20}$$

where

$$\mathrm{H}(s) = \mathrm{Diag}(\mathrm{w_S S}, \mathrm{w_T T}) \tag{21}$$

The details are well defined in the publication of Gahinet and Akparian (2011).

On solving the H_∞ optimization problem, the following controllers were obtained:

$$g_{c1} = \left(\frac{26.6s+0.104}{s}\right), g_{c2} = \left(\frac{33.4s+0.186}{s}\right) \tag{22}$$

Again, the setpoint tracking manipulated and controlled variable plots of the experimental and simulation results for the implementation of the controllers of (22) are shown in Figure 7. As was the case in Figure 6, the plots are strikingly similar.

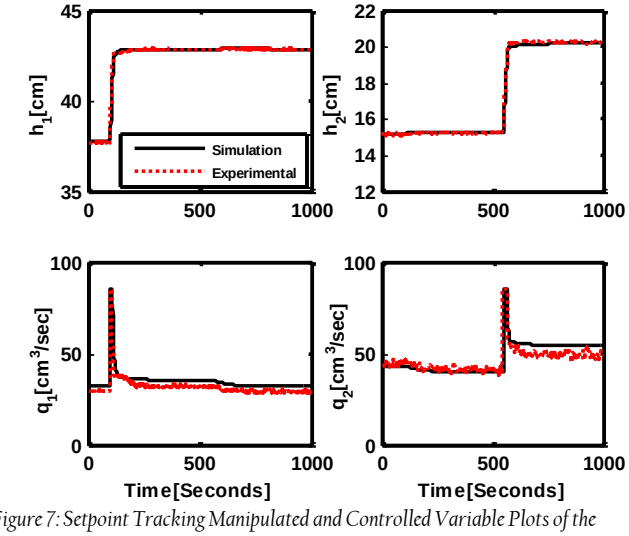

Figure 7: Setpoint Tracking Manipulated and Controlled Variable Plots of the Experimental and Simulation Results for the Implementation of the Fixed-Structure H_∞ Controllers of (22)

4.3. Multivariable Internal Model Controller (MIMC) design

A MIMC controller is designed by the inversion of the transfer function matrix of (13) and the subsequent augmentation of the inverse with a matrix of first-order filters i.e.

$$G_{IMC} = G^{-1}G_f \tag{23}$$

where

$$G_f = \begin{bmatrix} \frac{1}{\lambda_1 s+1} & 0 \\ 0 & \frac{1}{\lambda_2 s+1} \end{bmatrix} \tag{24}$$

By converting the G_{IMC} to a conventional feedback controller, G_c we obtained

$$G_c = \frac{G_{IMC}}{I-G_{IMC}G} = \begin{bmatrix} k_{11} & k_{12} \\ k_{21} & k_{22} \end{bmatrix} \tag{25}$$

where each controller k_{ij} $(i = 1,2; j = 1,2)$ is an 8th-order controller. The details are contained in Ogunba (2012).

Again, the plots of the manipulated and controlled variables of the implementation of the controllers of (25) are compared in Figure 8. The similarities are again noteworthy.

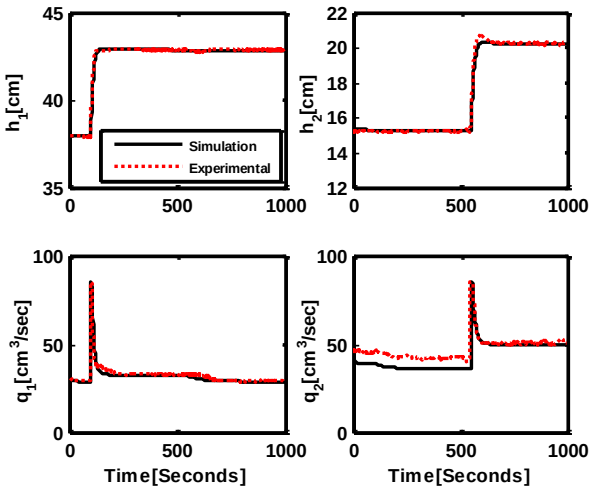

Figure 8: Setpoint Tracking Manipulated and Controlled Variable Plots of the Experimental and Simulation Results for the Implementation of Multivariable Internal Model Controllers of (25)

4.4. Simplified Decoupling Technique

Using the Decoupler Matrix $D(s)$ of (26) in the Simplified Decoupling framework (Waller, 1974; Waller *et al.*, 2003) yields an apparent process $Q(s)$ of (27) i.e.

$$D(s) = \begin{bmatrix} 1 & -\frac{g_{12}(s)}{g_{11}(s)} \\ -\frac{g_{21}(s)}{g_{22}(s)} & 1 \end{bmatrix} \tag{26}$$

$$Q(s) = \begin{bmatrix} g_{11}(s) - \frac{g_{12}(s)g_{21}(s)}{g_{22}(s)} & 0 \\ 0 & g_{22}(s) - \frac{g_{12}(s)g_{21}(s)}{g_{11}(s)} \end{bmatrix} \tag{27}$$

Using Single-Input, Single-Output Internal Model Control to generate SISO controllers and then converting the controllers to conventional unity feedback controllers yield the controllers of (28)

$$C(s) = \begin{bmatrix} c_{11}(s) & 0 \\ 0 & c_{22}(s) \end{bmatrix} \tag{28}$$

where each controller c_{ii} $(i = 1,2)$ is a 10th-order controller.

The multivariable controller is then given by (29)

$$G_c = D(s)C(s) \tag{29}$$

The plots of the manipulated and controlled variables of the implementation of the decoupler of (26) and the controllers of (28) are again compared in Figure 9. The similarities are again noteworthy.

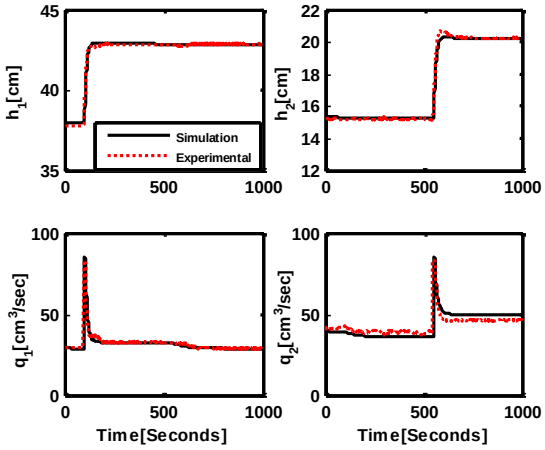

Figure 9: Set-point Tracking Manipulated and Controlled Variable Plots of the Experimental and Simulation Results for the Implementation of Simplified Decoupling Controllers of (26) and (28)

4.5. Model Predictive Controller Design

A MPC control problem consists of minimizing the cost function (Maciejowski, 2002 and Bamimore *et al*., 2011):

$$J(k) = \sum_{i=0}^{H_p-1} \|\hat{y}(k+i|k) - r(k+i|k)\|_Q^2 \quad + \sum_{i=0}^{H_u-1} \|\Delta\hat{u}(k+i|k)\|_R^2 \tag{30}$$

where $\hat{y}(k+i|k)$ are the predicted controlled outputs at time k, $\Delta u(k+i|k)$ are the predicted control increments, $r(k+i|k)$ are the set-point trajectories. The matrices $Q \geq 0$ and $R > 0$ are the weighing matrices, which are assumed to be constant over the prediction horizon. H_p is the length of the prediction horizon while H_u is the length of the control horizon.

On solving the optimization problem posed in equation (30), with the tuning parameters and process constraints specified as:

$H_p = 10$, $H_u = 2$, Q=diag([5,5]), R=0.005diag([1,1]), $\Delta q_{max} = \begin{bmatrix}10\\10\end{bmatrix}$, $\Delta q_{min} = \begin{bmatrix}-10\\-10\end{bmatrix}$, $q_{max} = \begin{bmatrix}85\\85\end{bmatrix}$, $q_{min} = \begin{bmatrix}0\\0\end{bmatrix}$, $h_{max} = \begin{bmatrix}62\\62\end{bmatrix}$, $h_{min} = \begin{bmatrix}0\\0\end{bmatrix}$,

a 9th-order controller is obtained. The details are contained in the appendix.

Again, the plots of the manipulated and controlled variables of the implementation of the controllers of are compared in Figure 10.

5. Conclusions

The experimental set-up of a laboratory-scale three-tank system of the Process System Engineering (PSE) Laboratory of Obafemi Awolowo University, Ile-Ife, Nigeria has been described. The usefulness of the set-up for the demonstration of advanced control laws has also been demonstrated with the design and implementation of popular control algorithms in literature. The striking similarities between controller implementations using SIMULINK and implementations on the real experimental set-up are noteworthy, with the major differences being in the noise introduced by the nonlinearities in the respective pumps. This set-up provides a massive opportunity for a practical demonstration of known control principles to engineering students.

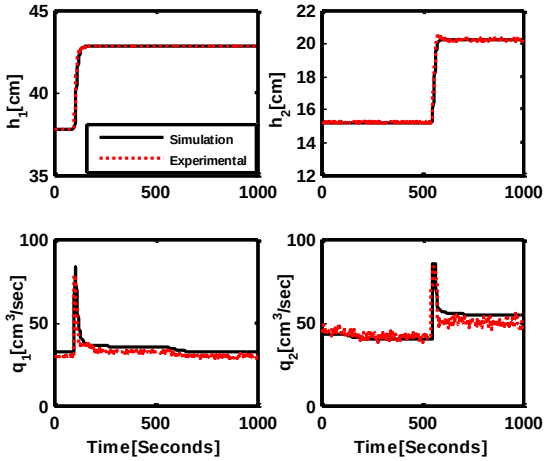

Figure 10: Set-point Tracking Manipulated and Controlled Variable Plots of the Experimental and Simulation Results for the Implementation of Linear Model Predictive Controllers of (31)

Acknowledgement

Prof. O. Taiwo acknowledges the donation of the Experimental System by Alexandria von Humbolt Foundation, Germany.

References

Bamimore, A., Taiwo, O. and King, R., "A Comparison of Two Nonlinear Model Predictive Control Methods and Implementation on a Laboratory Three Tank System." Proceedings of the 50th IEEE CDC-ECC Conference, 5242-5247, 2011.

Gahinet, P. and Apkarian, P., "Decentralized and Fixed-Structure H_∞Control in MATLAB." Proceedings of the 50th IEEE CDC-ECC Conference, 8205-8210, 2011.

Garrido, J., Vazquez, F., and Morilla, F., "Centralized Multivariable Control by Simplified Decoupling." Journal of Process Control, 22(6): 1044-1062, 2012.

Gatzke, E.P., Meadows, E.S., Wang, C., and Doyle III, F.J., "Model-Based Control of a Four-Tank System." Computers and Chemical Engineering, 24:1503-1509, 2000.

Goodwin, G. C., Graebe, S. F., and Salgado, M. E., "Control System Design", Prentice-Hall, Englewood Cliffs, New-Jersey, USA, 2000.

Johansson, K. H., "The Quadruple-Tank Process : A Multivariable Laboratory Process with an Adjustable Zero." IEEE Trans. Cont. Sys. Tech., 8 (3):456-465, 2000.

Klinkhieo, S. and Patton, R.J., "PLS based FDI of a Three-Tank Laboratory System." Proceedings of Joint 48th IEEE conference on Decision and Control and 28th Chinese Control Conference, Shanghai, China, 1896-1901, 2009.

Kovacs, L., Borbely, E., Benyo, Z., "Optimal control of the Three Tank System in H2/H-Inf Space." Fifth Slovakian-Hungarian Joint Symposium on Applied Machine Intelligence and Informatics, Poprad, Slovakia, 137-144, 2007.

Lincon, S.A., Sivakumar, D., Prakash, J., "State and Fault Parameter Estimation Applied To Three-Tank Bench Mark Relying On Augmented State Kalman Filter." ICGST-ACSE Journal, 7 (1):33-41, 2007.

Maciejowski, J. M., "Predictive Control with Constraints", Prentice-Hall, Harlow, England, 2002.

Ogunba, K. S., "Development of Generalized Internal Model Control (IMC) Techniques for Multivariable Control System Design." Unpublished M.Sc. Thesis, Obafemi Awolowo University, Ile-Ife, Nigeria, 2012.

Ogunleye, M. A., "Design of Controllers for Multivariable Systems using the Method of Inequalities." Unpublished M.Sc. Thesis, Obafemi Awolowo University, Ile-Ife, Nigeria, 2012.

Shneiderman, D. and Palmor, Z. J., "Properties and Control of the Quadruple-Tank Process with Multivariable Dead-Times." Journal of Process Control, 20:18-28, 2010.

Suresh, M., Srinivasan, G. J., Hemamalini, R. R., "Integrated Fuzzy Logic Based Intelligent Control of Three Tank System." Serbian Journal of Electrical Engineering, 6 (1):1-14, 2009.
Taiwo, O., "Improvement of Turbo-Alternator Response by the Method of Inequalities." International Journal of Control, 27 (2):305-311, 1978.
Taiwo, O. , "Application of The Method of Inequalities to the Multivariable Control of Binary Distillation Columns." Chem. Eng. Sci., 35 (2): 847-858, 1980.
Vadigepalli, R., Gatzke, E.P. and Doyle III, F.J., "Robust Control of a Multivariable Experimental Four-Tank System." Ind. Eng. Chem. Res., 40:1916-1927, 2001.
Waller, K. V., "Decoupling in Distillation." AIChE J., 20, 592-594, 1974.
Waller, M., Waller, J.B., and Waller, K.V., "Decoupling Revisited." Ind. Eng. Chem. Res. 42:4575-4577, 2003.
Wu, L., Cartes, D., Shih, C., "Web-Based Flow Control of a Three-Tank System." Journal of Systemics, Cybernetics and Informatics, 2(1): 242-251, 2003.
Zakian, V. and Al-Naib, U., "Design of Dynamical and Control Systems by the Method of Inequalities." Proc. IEE, 120 (11):1421-1427, 1973.

APPENDIX

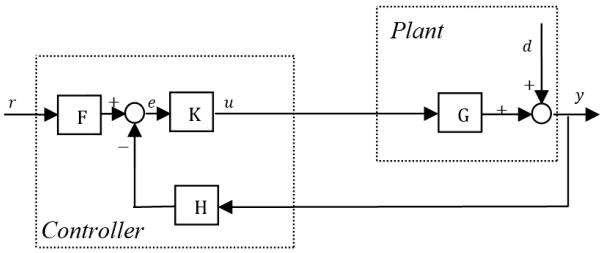

Block diagram describing the structure of a linear model predictive control system

MPC CONTROLLER

$$K = \begin{bmatrix} k_{11} & k_{12} \\ k_{21} & k_{22} \end{bmatrix}$$

$$k_{11} = \frac{s^9 + 17.64s^8 + 144.6 + 710s^6 + 2334s^5 + 5391s^4 + 8808s^3 + 9361s^2 + 6153s + 125.5}{s^9 + 17.83s^8 + 148.9s^7 + 752.3s^6 + 2570s^5 + 6211s^4 + 10640s^3 + 11930s^2 + 8101s + 147.2}$$

$$k_{21} = \frac{0.002317s^8 + 0.03207s^7 + 0.1747s^6 + 0.3497s^5 - 0.3977s^4 - 2.732s^3 - 1.883s^2 + 6.339s + 12.69}{s^9 + 17.83s^8 + 148.9s^7 + 752.3s^6 + 2570s^5 + 6211s^4 + 10640s^3 + 11930s^2 + 8101s + 147.2}$$

$$k_{12} = \frac{0.002348s^8 + 0.0325s^7 + 0.177s^6 + 0.3539s^5 - 0.4059s^4 - 2.778s^3 - 1.925s^2 + 6.405s + 12.85}{s^9 + 17.83s^8 + 148.9s^7 + 752.3s^6 + 2570s^5 + 6211s^4 + 10640s^3 + 11930s^2 + 8101s + 147.2}$$

$$k_{22} = \frac{s^9 + 17.63s^8 + 144.7s^7 + 712s^6 + 2351s^5 + 5467s^4 + 9007s^3 + 9652s^2 + 6355s + 127}{s^9 + 17.83s^8 + 148.9s^7 + 752.3s^6 + 2570s^5 + 6211s^4 + 10640s^3 + 11930s^2 + 8101s + 147.2}$$

$$F = \begin{bmatrix} \frac{1.266s+3.706}{s} & \frac{0.01324s+0.00244}{s} \\ \frac{0.0117s+0.002154}{s} & \frac{1.296s+3.799}{s} \end{bmatrix}, \quad H = \begin{bmatrix} h_{11} & h_{12} \\ h_{21} & h_{22} \end{bmatrix}$$

$$h_{11} = \frac{5.56s^4+174s^3+502.2s^2+47.29s+0.8235}{s^4+6.225s^3+9.758s^2+0.222s}, \qquad h_{21} = \frac{0.003231s^4+1.424s^3+4.466s^2+0.2452s+0.0004787}{s^4+6.225s^3+9.758s^2+0.222s}$$

$$h_{12} = \frac{0.00366s^4+1.443s^3+4.522s^2+0.3178s+0.0005422}{s^4+6.225s^3+9.758s^2+0.222s}, \qquad h_{22} = \frac{5.7s^4+165.6s^3+473s^2+47.54s+0.8443}{s^4+6.225s^3+9.758s^2+0.222s}$$

MIMC CONTROLLER

$$k_{11} = \frac{1.99e15s^8 + 2.75e14s^7 + 1.54e13s^6 + 4.48e11s^5 + 7.17e9s^4 + 6.18e7s^3 + 265624s^2 + 535.2s + 0.4045}{1.538e14s^8 + 1.987e13s^7 + 1.016e12s^6 + 2.638e10s^5 + 3.634e8s^4 + 2.494e6s^3 + 7002s^2 + 6.661s}$$

$$k_{21} = \frac{-1.8e11s^6 - 1.966e10s^5 - 8.08e8s^4 - 1.53e7s^3 - 131149s^2 - 405.6s - 0.4045}{1.538e14s^8 + 1.987e13s^7 + 1.016e12s^6 + 2.638e10s^5 + 3.634e8s^4 + 2.494e6s^3 + 7002s^2 + 6.661s}$$

$$k_{12} = \frac{-1.8e11s^6 - 1.966e10s^5 - 8.08e8s^41.53e7s^3 - 131149s^2 - 405.6s - 0.4045}{1.538e14s^8 + 1.987e13s^7 + 1.016e12s^6 + 2.638e10s^5 + 3.634e8s^4 + 2.494e6s^3 + 7002s^2 + 6.661s}$$

$$k_{22} = \frac{2.048e15s^8 + 3.157e14s^7 + 2e13s^6 + 6.78e11s^5 + 1.31e10s^4 + 1.42e8s^3 + 818511s^2 + 2083s + 1.871}{1.538e14s^8 + 1.987e13s^7 + 1.016e12s^6 + 2.638e10s^5 + 3.634e8s^4 + 2.494e6s^3 + 7002s^2 + 6.661s}$$

SIMPLIFIED DECOUPLER

$$k_{11} = \frac{5.44e19s^{10} + 9.1e18s^9 + 6.44e17s^8 + 2.51e16s^7 + 5.89s^6 + 8.48e12s^5 + 7.4e10s^4 + 3.78e8s^3 + 1.1e6s^2 + 1644s + 1}{3.4e18s^{10} + 5.35e17s^9 + 3.53e16s^8 + 1.27e15s^7 + 2.69e13s^6 + 3.4e11s^5 + 2.47e9s^4 + 9.6e6s^3 + 1.82e4s^2 + 13.27s}$$

$$k_{12} = \frac{-5.83e17s^{10} - 1.16e17s^9 - 10e15s^8 - 4.85e14s^7 - 1.47e13s^6 - 2.85e11s^5 - 3.56e9s^4 - 2.75e7s^3 - 1.2e5s^2 - 264.5s - 0.22}{5e20s^{12} + 1.1e20s^{11} + 1.05e19s^{10} + 5.8e17s^9 + 2.06e16s^8 + 4.86e14s^7 + 7.73e12s^6 + 8.19e10s^5 + 5.55e8s^4 + 2.22e8s^3 + 4528s^2 + 3.56s}$$

$$k_{21} = \frac{-5.44e19s^{10} - 9.1e18s^9 - 6.44e17s^8 - 2.51e16s^7 - 5.9e14s^6 - 8.5e12s^5 - 7.4e10s^4 - 3.78e8s^3 - 1.1e6s^2 - 1644s - 1}{3.76e22s^{12} + 7e21s^{11} + 5.66e20s^{10} + 2.6e19s^9 + 7.39e17s^8 + 1.36e16s^7 + 1.63e14s^6 + 1.24e12s^5 + 5.7e9s^4 + 1.56e7s^3 + 2.25e4s^2 + 13.27s}$$

$$k_{22} = \frac{2.7e18s^{10} + 5.36e17s^9 + 4.61e16s^8 + 2.25e15s^7 + 6.8e13s^6 + 1.32e12s^5 + 1.65e10s^4 + 1.27e8s^3 + 5.6e5s^2 + 1224s + 1}{2.03e17s^{10} + 3.52e16s^9 + 2.59e15s^8 + 1.05e14s^7 + 2.58e12s^6 + 3.88e10s^5 + 3.5e8s^4 + 1.76e6s^3 + 4135s^2 + 3.56s}$$